Printed in the Republic of Korea
ANALYTICAL SCIENCE & TECHNOLOGY
Vol. 37 No. 1, 39-46, 2024
https://doi.org/10.5806/AST.2024.37.1.39

Enhanced alizarin removal from aqueous solutions using zinc Oxide/Nickel Oxide nano-composite

Basma E. Jasim[1], Ali J. A. Al-Sarray[2,★], and Rasha M. Dadoosh[2]

[1]Department of Chemical Industrial, Institute of Technology/Baghdad, Middle Technical University, Baghdad, Iraq
[2]Polymer Research Unit, College of Science, Mustansiriyah University, Baghdad, Iraq

(Received October 19, 2023; Revised December 16, 2023; Accepted December 21, 2023)

Abstract: Alizarin dye, a persistent and hazardous contaminant in aquatic environments, presents a pressing environmental concern. In the quest for efficient removal methods, adsorption has emerged as a versatile and sustainable approach. This study focuses on the development and application of Zinc Oxide/Nickel Oxide (ZnO/NiO) nano-composites as adsorbents for alizarin dye removal. These semiconducting metal oxide nano-composites exhibit synergistic properties, offering enhanced adsorption capabilities. Key parameters affecting alizarin removal, such as contact time, adsorbent dosage, pH, and temperature, were systematically investigated. Notably, the ZnO/NiO nano-composite demonstrated superior performance, with a maximum alizarin removal percentage of 76.9 % at pH 6. The adsorption process followed a monolayer pattern, as suggested by the Langmuir model. The pseudo-second-order kinetics model provided a good fit to the experimental data. Thermodynamic analysis indicated that the process is endothermic and thermodynamically favorable. These findings underscore the potential of ZnO/NiO nano-composites as effective and sustainable adsorbents for alizarin dye removal, with promising applications in wastewater treatment and environmental remediation.

Key words: alizarin dye removal, adsorption, environmental remediation, water treatment, nano-composite

1. Introduction

Alizarin dye (*Fig.* 1), a representative synthetic dye commonly employed in textile industries, poses a significant environmental concern due to its persistence in aquatic environments.[1,2] The textile industry alone annually contributes an estimated 280,000 tons of synthetic dyes to water bodies worldwide,[3] primarily comprising recalcitrant compounds like alizarin dye. Alizarin dye, recognized for its hazardous nature, exhibits mutagenic and carcinogenic properties, exacerbating its environmental impact.[4-6]

The removal of alizarin dye from aqueous solutions has necessitated the exploration of various methods. Among these, adsorption has garnered substantial attention for its capacity to effectively sequester alizarin dye molecules from solution.[7,8] Adsorption's appeal is rooted in its versatility, cost-efficiency, and applicability across a wide spectrum of dyes, including alizarin.[9]

★ Corresponding author
Phone : +964-(0)77-1634-3326
E-mail : ali_alsarray@uomustansiriyah.edu.iq

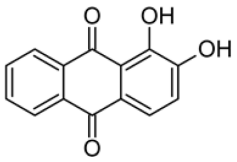

Fig. 1. The chemical structure of alizarin compound.

Notably, adsorption circumvents the issue of generating secondary pollutants, a concern often associated with alternative treatment methods.[10] Alizarin dye removal via adsorption is particularly advantageous at low concentrations, making it applicable to both industrial effluents and environmental remediation efforts.[11,12] Furthermore, adsorption permits flexibility through the selection of suitable adsorbents and the optimization of operational parameters, rendering it an adaptable solution.[13]

Recent research has explored the potential of nanoparticles, specifically nanosized metal oxides such as cerium oxide, magnesium oxide, ferric oxide, and manganese oxides, as effective adsorbents for alizarin dye.[14,15] These nanomaterials offer a large surface area, abundant active sites, and tunable surface chemistry, thereby enhancing the interaction with alizarin dye molecules.[16,17]

Utilizing nanosized metal oxides for alizarin dye adsorption presents distinct advantages. The high surface area-to-volume ratio of nanoparticles facilitates efficient adsorption even at low alizarin dye concentrations.[16,18] Additionally, facile synthesis and functionalization methods can further enhance their adsorption performance, making them versatile adsorbents for alizarin dye and related compounds.[19,20] Moreover, the reusability, cost-effectiveness, and minimal environmental impact of nanosized metal oxides underscore their potential as sustainable solutions for alizarin dye removal.[21,22]

This work focuses on the development and application of Zinc Oxide/Nickel Oxide (ZnO/NiO) nanocomposites as proficient adsorbents for alizarin dye removal. These semiconducting metal oxides, when combined into a nano-composite, exhibit synergistic properties that can be harnessed for enhanced alizarin dye removal from aqueous solutions.[23,24] The primary objective of this research is to synthesize and characterize ZnO/NiO nano-composites tailored specifically for alizarin dye adsorption under diverse conditions.

2. Experimental

2.1. Chemicals and reagents

We utilized zinc oxide nanoparticles (ZnO-NPs) and nickel oxide nanoparticles (NiO-NPs), both of which had been synthesized according to the methods detailed in previous studies.[25,26] These nanoparticles, obtained with the same specifications as previously reported, played essential roles in the current study and were used without further purification.

2.2. Preparation of NiO/ZnO nano-composite

The synthesis of the NiO/ZnO nano-composite involved series of steps. Initially, ZnO-NPs and NiO-NPs were combined in appropriate concentrations, followed by the addition of distilled water to the mixture. Subsequently, the mixture was subjected to one-hour sonication to ensure proper dispersion. The resulting suspension was then dried overnight in an oven to form a precipitate, which was subsequently ground to a fine powder. Lastly, the dried precipitate was calcinated at 650 °C for a duration of four hours to yield the final NiO/ZnO nano-composite material.

2.3. The experiments of adsorption

The adsorption studies were carried out in 100 mL airtight Erlenmeyer flasks using a fixed volume of 50 mL of 10 $mg \cdot L^{-1}$ alizarin solution at a constant temperature of 25 °C. A consistent amount of the nano-composite adsorbent was introduced, and the effects of adsorbent dosage (0.02 to 0.1 g) and contact time (0 to 100 min) were investigated while maintaining a constant initial alizarin concentration of 10 $mg \cdot L^{-1}$. Temperature effects (20 to 40 °C) were examined with a fixed adsorbent dose of 0.02 g. The impact of pH (ranging from 2 to 14) on alizarin adsorption was studied by adjusting the initial pH of the solution using HCl and NaOH solutions. Quantification of adsorbed alizarin was performed at 550 nm using a UV-vis spectrometer, and all experiments

were conducted with continuous mixing to ensure uniform conditions. The adsorption capacity (q_e) was calculated using Eq. (1), while Eq. (2) is used to calculate the removal percentage (R%) of the dye[27]:

$$qe = \frac{(C_i - C_f)}{w} \times V \quad (1)$$

$$R\% = \frac{(C_i - C_f)}{C_i} \times 100 \quad (2)$$

Where C_i (mg·L^{-1}) represents the initial concentration, C_f (mg·L^{-1}) is the final concentration of alizarin, V (L) denotes the volume of the mixture, and w (g) signifies the weight of the adsorbent.

2.4. adsorption isotherm

In order to comprehensively elucidate the adsorption behavior of alizarin dye onto the nano-composite adsorbent, three well-established isotherm models were employed: Freundlich, Langmuir, and Tempkin models.

The Freundlich isotherm model was utilized to assess the adsorption process. The model is described by Eq. (3), which represents the linearized form of the Freundlich model[28]:

$$\log q_e = \log K_f + \frac{1}{n} \log C_e \quad (3)$$

Here, (q_e) signifies the equilibrium adsorption capacity (mg·g^{-1}), (C_e) denotes the equilibrium concentration of alizarin (mg·L^{-1}), (K_f) is the Freundlich constant related to adsorption capacity (mg·g^{-1}), and (n) represents the Freundlich intensity factor, providing insights into the adsorption mechanism.

The Langmuir model was employed to ascertain the monolayer adsorption capacity and affinity of the nano-composite for alizarin dye. Eq. (4) describes the Langmuir isotherm model[29]:

$$q_e = \frac{q_{max} b C_e}{(1 + bC_e)} \quad (4)$$

In this equation, (q_{max}) signifies the maximum adsorption capacity (mg·g^{-1}), and (b) stands for the Langmuir affinity coefficient (L·mg^{-1}). Eq. (5) illustrates the linearized form of the Langmuir model:

$$\frac{1}{q_e} = \frac{1}{(bq_{max} C_e)} + \frac{1}{q_{max}} \quad (5)$$

The Temkin isotherm model offers valuable information about indirect adsorbate-adsorbent interactions and adsorption energetics. The model is represented by Eq. (6)[30]:

$$q_e = \frac{A}{B} \ln(AC_e) \quad (6)$$

where (B) is the Temkin constant (L·g^{-1}), and (A) is the equilibrium binding energy (J·mol^{-1}). (A) and (B) are Temkin model parameters that provide insights into the adsorption process, including the heat of adsorption and the interaction between the adsorbate and adsorbent. By fitting experimental data to these three models, valuable information regarding the adsorption mechanism and energetics can be obtained.

2.5. Adsorption kinetics

To investigate the kinetics of alizarin dye adsorption onto the nano-composite adsorbent, a series of experiments were conducted in 100 mL conical flasks at pH 2. In each flask, 0.05 g of the adsorbent was mixed with 50 mL of alizarin solution (10 mg·L^{-1}). The mixtures were agitated at room temperature for varying time intervals of 10, 20, 30, 40, 50, and 60 min. The adsorption kinetics data were analyzed using the pseudo-second-order kinetic model, represented by Eq. (7):

$$\frac{t}{q_t} = \frac{1}{K_2 q_2^2} + \frac{t}{q_e} \quad (7)$$

Where (q_t) represents the amount of alizarin dye adsorbed at time (t) (mg·g^{-1}), (q_e) is the equilibrium adsorption capacity (mg·g^{-1}), and (K_2) signifies the second-order rate constant (g·mg^{-1}·min). To obtain a linear relationship for the kinetics of the adsorbed dye at time (t), a plot was constructed with (t/q_t) on the y-axis and (t) on the x-axis. The slope and intercept of this plot yielded the values of (K_2) and (q_e), respectively.

2.6. Adsorption thermodynamics

To understand the thermodynamic aspects of the

adsorption process and evaluate its spontaneity, a thorough thermodynamic analysis was conducted. This analysis aimed to elucidate the enthalpy change (ΔH, kJ·mol^{-1}), entropy change (ΔS, J·mol^{-1}·K^{-1}), and Gibbs free energy change (ΔG, kJ·mol^{-1}) associated with the adsorption of alizarin dye onto the nano-composite adsorbent.

To obtain these thermodynamic parameters, experiments were carried out at different temperatures, specifically, 30, 40, and 50 °C. The values of ΔH and ΔS were determined from the slope and intercept, respectively, of a plot constructed using Eq. (8), while the Gibbs free energy change (ΔG) was calculated using Eq. (9):

$$\ln K_d = \frac{\Delta S^o}{R} - \frac{\Delta H^o}{RT} \quad (8)$$

$$\Delta G^o = \Delta H^o - T\Delta S^o \quad (9)$$

Where (T) represents the absolute temperature (K), (R) stands for the universal gas constant (8.314 J·mol^{-1}·K^{-1}), and (K_d) signifies the equilibrium constant which equals to $\frac{q_e}{C_e}$.

3. Results and Discussion

3.1. Calibration data for alizarin absorbance

The calibration data in (*Fig.* 2) demonstrate a strong positive correlation between alizarin concentration and absorbance. As the concentration of alizarin increases, the absorbance values also increase, indicating

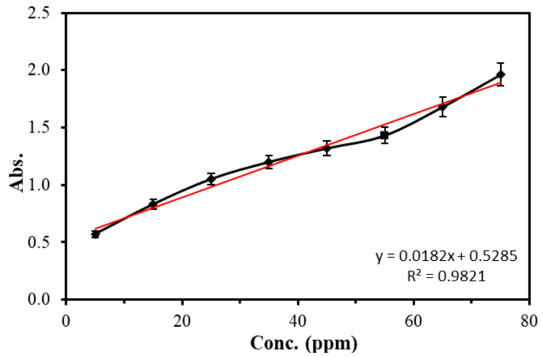

Fig. 2. Calibration curve of the alizarin absorbance at different concentration.

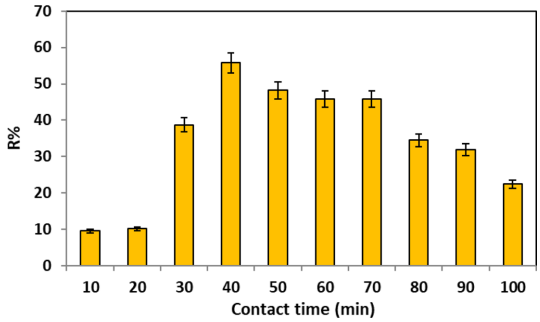

Fig. 3. The effect of contact time on the removal of alizarin by ZnO/NiO nanocomposite.

a proportional relationship. This calibration curve is essential for quantifying the concentration of alizarin in subsequent experiments.

3.2. Contact time

The time-dependent adsorption efficiency results (*Fig.* 3) indicate that the removal percentage (R%) of alizarin increases significantly with time, reaching a maximum of approximately 55.8 % after 40 minutes of contact with the adsorbents. This initial rise in R% can be attributed to the dynamic nature of the adsorption process, wherein extended contact times allow for the occupation of active sites on the adsorbent surface, leading to increased alizarin removal. However, beyond 40 minutes, a subsequent decrease in R% is observed. This decline could be elucidated by considering the establishment of an equilibrium condition between the adsorption and desorption processes. It is conceivable that as the adsorption sites become increasingly saturated, desorption may become more prominent, resulting in a reduction in the overall removal efficiency.

3.3. Mass-dependent adsorption efficiency

Fig. 4 presents the mass-dependent adsorption efficiency data, revealing that the adsorbent mass has a substantial impact on alizarin removal. As the mass of the adsorbent increases, the removal percentage (R%) also increases, indicating that a higher mass of adsorbent provides more active sites for alizarin adsorption. This finding underscores the importance of optimizing the adsorbent dosage for practical

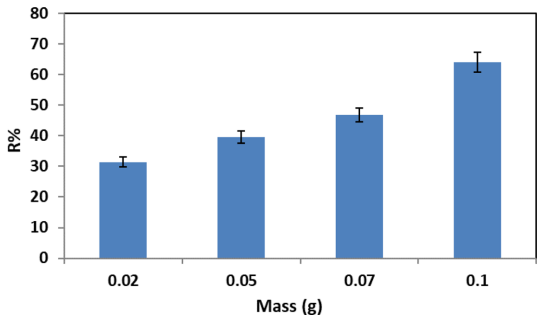

Fig. 4. The impact of adsorbent mass on the removal efficiency in terms of removal percentage.

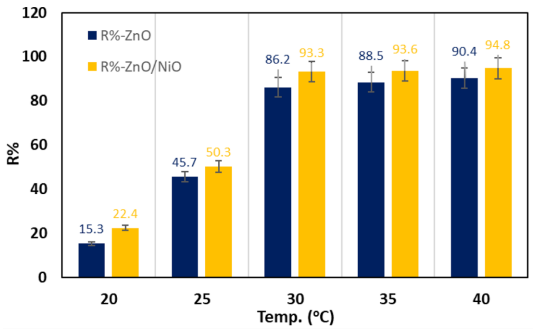

Fig. 5. The impact of temperature on the removal percentage for ZnO/NiO nanocomposite (R%-ZnO/NiO) and ZnO nanoparticle (R%-ZnO).

applications to achieve efficient alizarin removal.

3.4. pH-Dependent adsorption efficiency

The pH-dependent adsorption efficiency results in *Table* 1 demonstrate that the pH of the solution significantly influences alizarin removal. Alizarin removal is most effective at pH 6, with a removal percentage of 76.9 %, while lower and higher pH values result in reduced removal efficiencies. This pH-dependent behavior can be attributed to changes in the surface charge of the adsorbent and the ionization of alizarin, which affect adsorption interactions.

3.5. Temperature-dependent adsorption efficiency

Fig. 5 presents the temperature-dependent adsorption efficiency for both ZnO/NiO nanocomposite and ZnO nanoparticles. The results indicate that higher temperatures enhance alizarin removal efficiency. This suggests that the adsorption process is endothermic, and increased temperature provides more kinetic energy to the system, facilitating adsorption. Moreover, at each temperature point, the removal efficiency of ZnO/NiO is consistently higher than that of ZnO which may be due to synergistic effects between the two materials. This interpretation aligns with thermodynamic principles, providing insights into the temperature-driven dynamics of the adsorption process.

3.6. Adsorption isotherms

The analysis of adsorption isotherms using Langmuir (*Fig.* 6(a)), Freundlich (*Fig.* 6(b)), and Temkin (*Fig.* 6(c)) models helps in understanding the adsorption mechanisms. The Langmuir model suggests that the adsorption process follows monolayer adsorption, while the Freundlich model indicates heterogeneous adsorption. The Temkin model suggests that adsorption follows a non-linear pattern. These models provide valuable information for designing and optimizing adsorption processes for alizarin removal. The adsorption process followed a monolayer pattern, as suggested by the Langmuir model.

3.7. Adsorption kinetics

The chemical adsorption is expected to contain valence forces due to sharing or exchanging electrons between the adsorbent and alizarin dye which can be fitted in the pseudo-second-order equation.[31] Linear correlation was obtained by plotting (t/q_t) against (t) which conform that the adsorption process obeys the pseudo-second-order kinetics (*Fig.* 5). From the slope and intercept, the qe and k_2 parameters were 0.7290 ($mg \cdot g^{-1}$) and 0.2154 ($g \cdot mg^{-1} \cdot min^{-1}$), respectively.

Table 1. The effect of pH on the percentage of alizarin removal R%

pH	2	4	6	8	10	12	14
R%	32.4	34.9	76.9	22.5	21.0	18.3	20.0

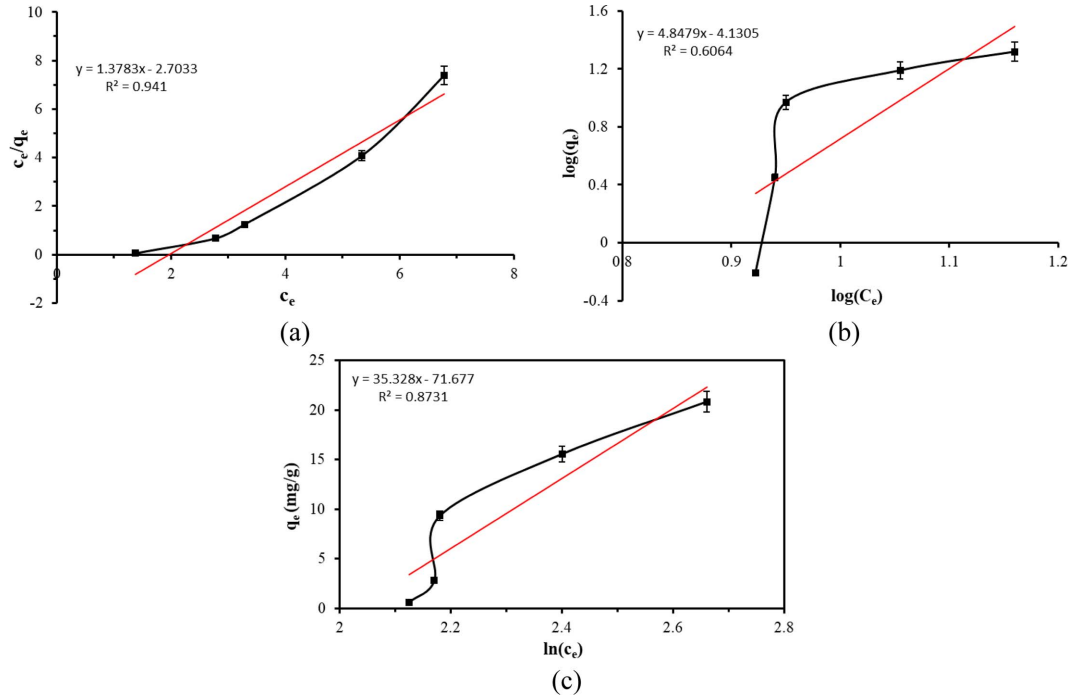

Fig. 6. Langmuir (a), Freundlich (b), and Temkin (c) Isotherms models of alizarin adsorption.

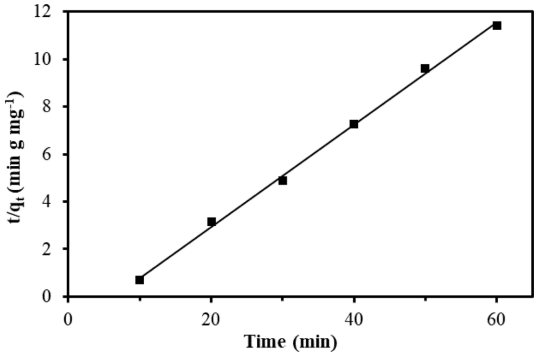

Fig. 7. Pseudo-second-order kinetics of adsorbing alizarin onto ZnO/NiO nanocomposite.

The correlation coefficient of this model is 0.998 which implies that there is a good correlation for alizarin dye adsorption onto ZnO/NiO nanocomposite. The high value of k_2 is due to the fact that the rate of adsorption in the pseudo-second-order model is proportional to empty sites number squared.[32]

3.8. Thermodynamic parameters

Table 9 presents the thermodynamic parameters, including ΔH, ΔG, and ΔS, which offer insights into the spontaneity and energetics of the adsorption process. The positive ΔH value indicates an endothermic process, and the negative ΔG values at various temperatures suggest that the adsorption of alizarin onto the adsorbents is thermodynamically favorable and suggest a physisorption process. The positive ΔS value suggests increased disorder during adsorption. These findings support the potential application of ZnO/NiO nanocomposite for alizarin removal.

Table 2. Thermodynamic factors of alizarin sorption onto ZnO/NiO nanocomposite

Temperature (°C)	ΔG^o (kJ·mol^{-1})	ΔH^o (kJ·mol^{-1})	ΔS^o (J·mol^{-1}·K^{-1})
30	-13.38		
40	-9.15	9.580	0.312
50	-4.93		

3.9. The significance of the results

This research not only contributes to the understanding of the fundamental characteristics of ZnO/

NiO nano-composites but also highlights their significant role in addressing water pollution challenges, particularly in the removal of persistent and hazardous contaminants such as alizarin dye from aquatic environments. The findings presented herein pave the way for the development of effective and sustainable adsorbents with broader implications for environmental protection and wastewater treatment.

4. Conclusions

In this study, we explored the efficacy of Zinc Oxide/Nickel Oxide (ZnO/NiO) nano-composites as adsorbents for the removal of alizarin dye from aqueous solutions. The investigation revealed that the ZnO/NiO nano-composite exhibited excellent performance in adsorbing alizarin, with a maximum removal percentage of 76.9 % achieved at pH 6. The adsorption process was governed by monolayer adsorption, as indicated by the Langmuir isotherm model and pseudo-second-order kinetics. Thermodynamic analysis showed that the adsorption process is endothermic and thermodynamically favorable, suggesting its potential for practical applications.

Acknowledgements

The authors would like to thank Mustansiriyah University (www.uomustansiriyah.edu.iq) Baghdad, Iraq for its support in the present work.

References

1. S. Rai, R. Saremi, S. Sharma, and S. Minko, *Green Chemistry*, **23**(20), 7937-7944 (2021). https://doi.org/10.1039/D1GC02043A
2. S. Benkhaya, S. M'rabet, H. Lgaz, A. El Bachiri, and A. El Harfi, *Dye Biodegradation, Mechanisms and Techniques: Recent Advances*, 1-50 (2022). https://doi.org/10.1007/978-981-16-5932-4_1
3. L. J. Rather, S. Jameel, O. A. Dar, S. A. Ganie, K. A. Bhat, and F. Mohammad, *Water in Textiles and Fashion*, **2019**, 175-194 (2019). https://doi.org/10.1016/B978-0-08-102633-5.00010-5
4. U. Shanker, M. Rani, and V. Jassal, *Environmental Chemistry Letters*, **15**, 623-642 (2017). https://doi.org/10.1007/s10311-017-0650-2
5. J. Wu, H. Zhao, M. Wang, W. Zhi, X. Xiong, and L. Zheng, *Fibers and Polymers*, **20**, 2376-2382 (2019). https://doi.org/10.1007/s12221-019-9029-2
6. A. J. A. Al-Sarray, T. Al-Kayat, B. M. Mohammed, M. J. B. Al-assadi, and Y. Abu-Zaid, *Journal of Medicinal and Chemical Sciences*, **5**(7), 1321-1330 (2022). https://doi.org/10.26655/JMCHEMSCI.2022.7.21
7. S. Al Arni, S. Ghareba, C. Solisio, M. S. Alves Palma, and A. Converti, *Environmental Engineering Science*, **38**(7), 577-591 (2021). https://doi.org/10.1089/ees.2020.0338
8. A. J. A. Al-Sarray, *Eurasian Chemical Communications*, **5**(4), 317-326 (2023). https://doi.org/10.22034/ecc.2023.374322.1565
9. R. Bushra, S. Mohamad, Y. Alias, Y. Jin, and M. Ahmad, *Microporous and Mesoporous Materials*, **319**, 111040 (2021). https://doi.org/10.1016/j.micromeso.2021.111040
10. Y. Zhou, J. Lu, Y. Zhou, and Y. Liu, *Environmental Pollution*, **252**, 352-365 (2019). https://doi.org/10.1016/j.envpol.2019.05.072
11. A. K. Badawi, M. Abd Elkodous, and G. A. Ali, *RSC Advances*, **11**(58), 36528-36553 (2021). https://doi.org/10.1039/D1RA06892J
12. A. M. Al-Khazraji, R. A. Al Hassani, and A. Ahmed, *Sys. Rev. Pharm.*, **11**(5), 525-534 (2020). http://dx.doi.org/10.31838/srp.2020.5.70
13. N. Kaya, *Water Science and Technology*, **76**(2), 478-489 (2017). https://doi.org/10.2166/wst.2017.216
14. S. Laurent, S. Boutry, and R. Muller, *Iron Oxide Nanoparticles for Biomedical Applications*, **3**, 42 (2018). https://doi.org/10.4155/fmc.09.164
15. A. Agrawal and K. Sahu, *Journal of Hazardous Materials*, **137**(2), 915-924 (2006). https://doi.org/10.1016/j.jhazmat.2006.03.039
16. S. R. Aqdam, D. E. Otzen, N. M. Mahmoodi, and D. Morshedi, *Journal of Colloid and Interface Science*, **602**, 490-503 (2021). https://doi.org/10.1016/j.jcis.2021.05.174
17. A. Al-Sarray, *Current Chemistry Letters*, **13**(1), 207-224 (2024). http://dx.doi.org/10.5267/j.ccl.2023.6.007
18. M. Rajeswari, K. Bhoomika, H. Ruksar, R. Naveen, S. Vidyadhara, N. N. Rao, and A. Sharma, *SPAST Abstracts*,

1(01), (2021). https://spast.org/techrep/article/view/1032
19. J. C. Cruz, M. A. Nascimento, V. A. Luciano, F. C. Souza, J. W. Oliveira, J. D. Ardisson, A. P. C. Teixeira, and R. P. Lopes, *Ceramics International*, **47**(3), 4357-4360 (2021). https://doi.org/10.1016/j.ceramint.2020.09.286
20. A. J. Al-Sarray, I. M. Al-Mussawi, T. H. Al-Noor, and Y. Abu-Zaid, *Journal of Medicinal and Chemical Sciences*, **5**(6), 1094-1101 (2022). https://doi.org/10.26655/JMCHEMSCI.2022.6.22
21. M. P. De Haan, N. Balakrishnan, A. R. Kuzmyn, G. Li, H. M. Willemen, G. Seide, G. C. Derksen, B. Albada, and H. Zuilhof, *Langmuir*, **37**(4), 1446-1455 (2021). https://doi.org/10.1021/acs.langmuir.0c02981
22. A. J. Al-Sarray, I. M. H. Al-Mousawi, and T. H. Al-Noor, *Chemical Methodologies*, **6**(4), 331-338 (2022). https://doi.org/10.22034/chemm.2022.328714.1439
23. A. Jawed, V. Saxena, and L. M. Pandey, *Journal of Water Process Engineering*, **33**, 101009 (2020). https://doi.org/10.1016/j.jwpe.2019.101009
24. E. Syahdarani, A. Ramelan, S. Wahyuningsih, A. Subagio, I. Kartini, and K. Kawuri, *Journal of Physics: Conference Series*, **2190**, 012015 (2022). https://doi.org/10.1088/1742-6596/2190/1/012015
25. N. A.-A. Aboud, W. M. Alkayat, and D. H. Hussain, *Drug Invention Today*, **13**(3), 81-87 (2020).
26. B. Jasim, A. A. Ahmed, and N. Aboud, *Baghdad Science Journal*, (2023). https://dx.doi.org/10.21123/bsj.2023.7516
27. K. M. Abualnaja, A. E. Alprol, M. Abu-Saied, A. T. Mansour, and M. Ashour, *Nanomaterials*, **11**(5), 1144 (2021). https://doi.org/10.3390/nano11051144
28. H. Freundlich. *Über die Adsorption in Lösungen. Habilitationsschrift durch welche... zu haltenden Probevorlesung* "*Kapillarchemie und Physiologie*" *einladet Dr. Herbert Freundlich*; W. Engelmann, 1906.
29. I. Langmuir, *Journal of the American Chemical Society*, **38**(11), 2221-2295 (1916). https://doi.org/10.1021/ja02268a002
30. M. R. R. Kooh, M. K. Dahri, and L. B. Lim, *Cogent Environmental Science*, **2**(1), 1140553 (2016). https://doi.org/10.1080/23311843.2016.1140553
31. A. David and L. Joseph. The Effect of Ph and Biomass Concentration on Lead (Pb) Adsorption by Aspergillus Niger from Simulated Waste Water. UMP, 2008.

Authors' Positions

Basma E. Jasim : Lecturer and Researcher
Ali J. A. Al-Sarray : Lecturer and Researcher
Rasha M. Dadoosh : Lecturer and Researcher